

Advanced Technology for Evaluation of Pore Structure Characteristics of Filtration Media to Optimize Their Design and Performance

Dr. Akshaya Jena and Dr. Krishna Gupta
Porous Materials, Inc.,
Ithaca, NY 14850

Contents

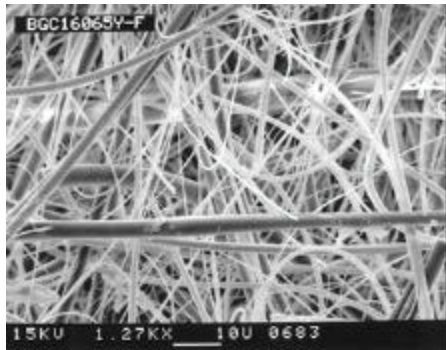
1. Pore Structure of Filtration Media
2. Characteristics of Pore Structure
3. Definition of Pore Diameter
4. Characterization Techniques
5. Extrusion Flow Porometry
 - 5.1 Principle
 - 5.2 Measurable characteristics
 - 5.3 Measurement of the effects of service environment
 - 5.4 Instrument
6. Extrusion Porosimetry
 - 6.1 Principle
 - 6.2 Measurable characteristics
 - 6.3 Instrument
7. Mercury Intrusion Porosimetry
 - 7.1 Principle
 - 7.2 Measurable characteristics
 - 7.3 Instrument
8. Non-Mercury Intrusion Porosimetry
9. Vapor Adsorption Technique
 - 9.1 Principle
 - 9.2 Measurable characteristics
 - 9.3 Instrument
10. Vapor Condensation Technique
 - 10.1 Principle
 - 10.2 Measurable characteristics
 - 10.3 Instrument
11. Capabilities of the Techniques
12. Examples of Applications
 - 12.1 Homogeneity of filtration media
 - 12.2 Design of composite filtration media
 - 12.3 Pore Structure of ceramic filtration medium
13. Summary and Conclusions
14. References

1. Pore Structure of Filtration Media

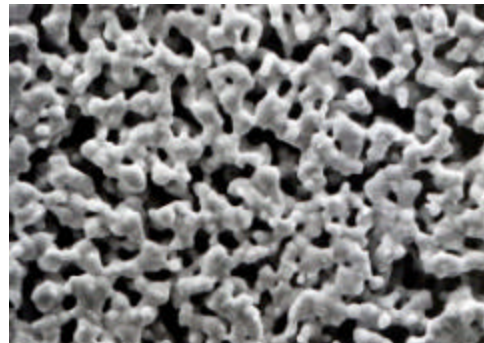
Pore structure of filtration media can be quite complex (Figure 1). Interconnected pores normally have irregular cross-sections that vary along pore path. The through pores extend from one side of filtration media to the another and permit fluid flow. The blind pores terminate inside the filtration media. These pores do not permit fluid flow, but blind pore surface area can adsorb gases, capture small particles and participate in reactions. The closed pores are not accessible. The pore structure may not be isotropic. The structure in the z-direction(thickness direction) can be considerably different from those in the x-y plane (plane perpendicular to the thickness direction). Characterization of such a complex pore structure requires specification of a number of characteristics.

2. Characteristics of Pore Structure

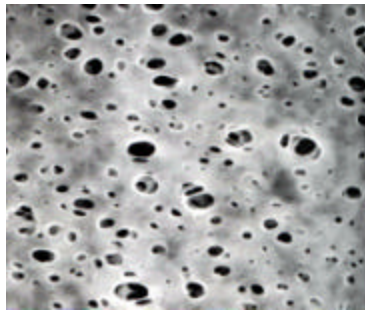
Size of particles that can not pass through filtration media is determined by the size of pores at their most constricted parts. Therefore, the largest, the mean and the range of the most constricted through pore sizes and the pore distributions are important characteristics that determine the barrier properties of filtration media. Pore volume is a measure of holding capacity. The through pore (envelope) surface area captures particles (Figure 1). The total surface area controls adsorption of gases and chemical reactions. The process rates are determined by liquid and gas permeability. Figure 2 lists the characteristics.



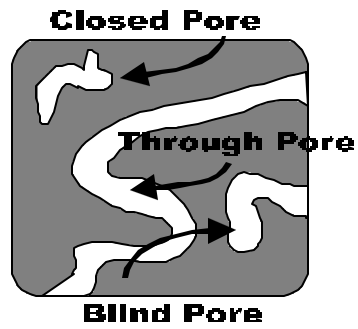
(a) Nonwoven



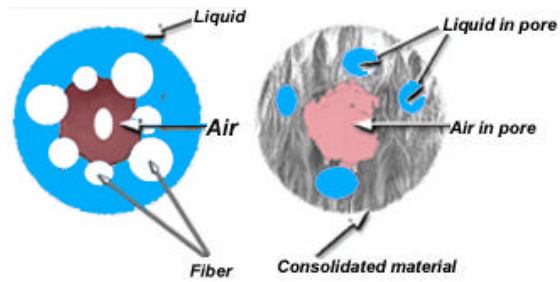
(b) Sintered stainless steel



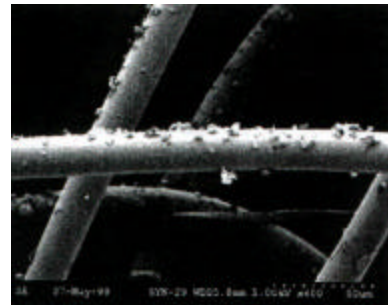
(c) Membrane



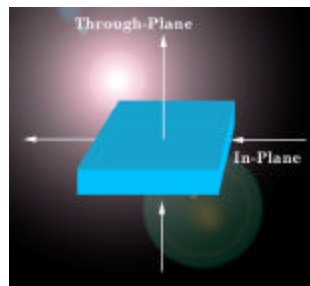
(d) Three kinds of pores



(e) Pore cross-section



(f) Pore surface



(g) x-y plane & z direction pores

Figure 1. Complex pore structure of filtration media.

Constricted through pore diameters

(The largest, Mean, Range & Distribution)

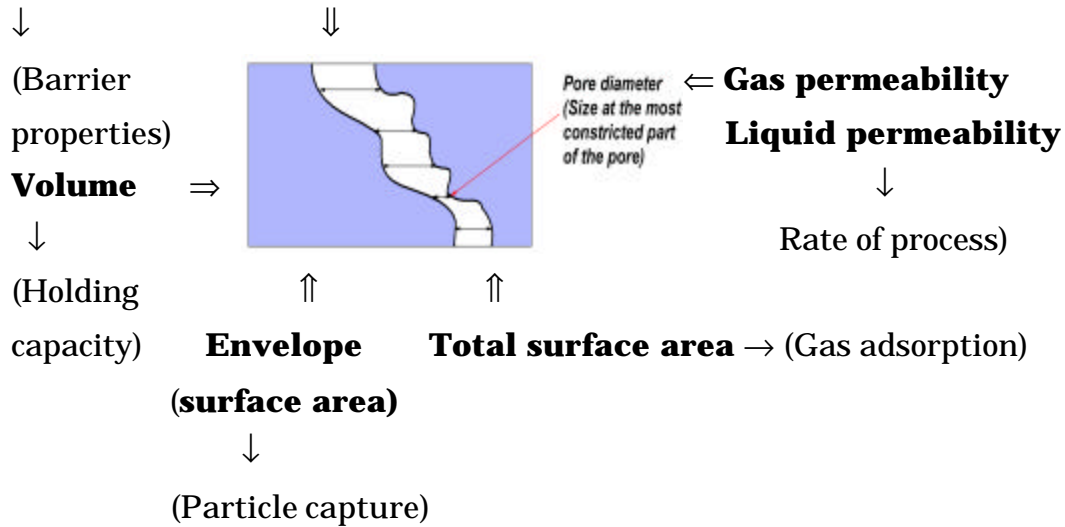


Figure 2. Important pore structure characteristics.

The application environment of filtration media is often considerably different from the test environment. The application environment can appreciably modify the pore structure. Therefore, effects of application environment on pore structure characteristics need to be determined. The important application environments are listed in Figure 3.

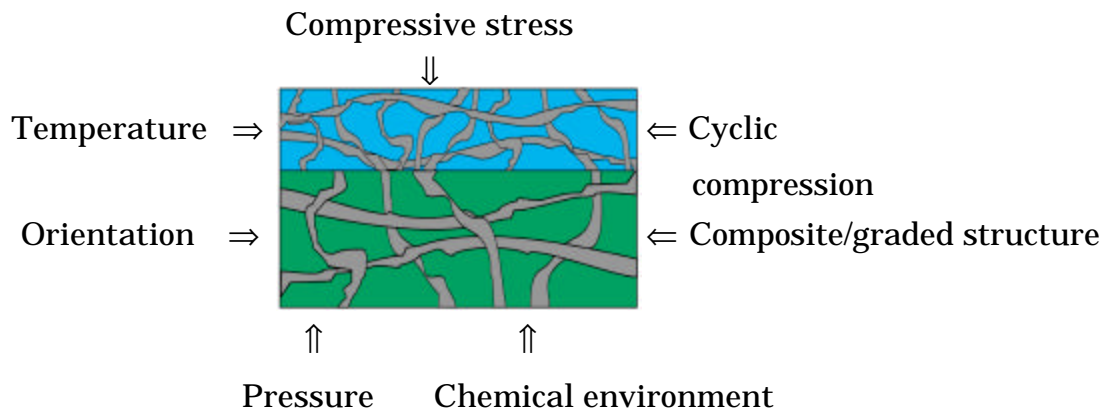


Figure 3. Effects of application environment on characteristics

3. Definition of Pore Diameter

Pore size is given in terms of pore diameter. However, a unique pore size cannot be specified for most of the pore cross-sections (Figures 4). Pore diameter needs to be defined.



Figure 4. Examples of pore cross-section

The diameter, D of a pore at any of its cross-section is defined in the following manner.

$$\begin{aligned}
 (dS/dV)_{\text{pore}} &= (dS/dV)_{\text{circular opening of diameter, } D} \\
 &= (4/D) \\
 &\Rightarrow (\text{Perimeter}) / (\text{Area})
 \end{aligned}
 \tag{1}$$

This is illustrated in Figure 5. Table 1 shows the relationships between measure pore diameters and actual pore size for a few pore cross-sections.

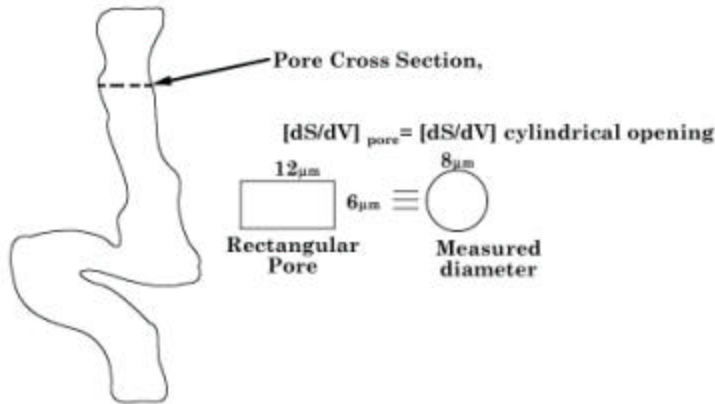

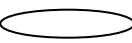
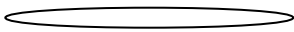

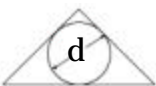
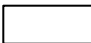


Figure 5. Definition of pore diameter

Table 1. Relation between measured pore diameter and actual pore size.

| Filtration media | Pore cross-section | Axial ratio | Shape factor, λ ($d = \lambda D$) |
|-----------------------|--------------------|---|--|
| Consolidated Material | Circular |  $n=1$ | 1 |
| | Elliptical |  $n=5$ | 0.72 |
| | Slit |  $n=5$ | 0.71 |
| Fibrous Material | Square |  $n=1$ | 1.0 |
| | Triangular |  $n=1$ | 1.0 |
| | Rectangular |  $n=2$ | 0.75 |

4. Characterization Techniques

Techniques like high resolution microscopy and x-ray microtomography can give a number of pore characteristics. However, tiny areas scanned by these techniques do not give average properties of macroscopic samples. These techniques are also expensive, time consuming and involved. We will consider here the techniques that are simple, fast, easy to use and inexpensive. The diagram in Figure 6 lists these techniques.

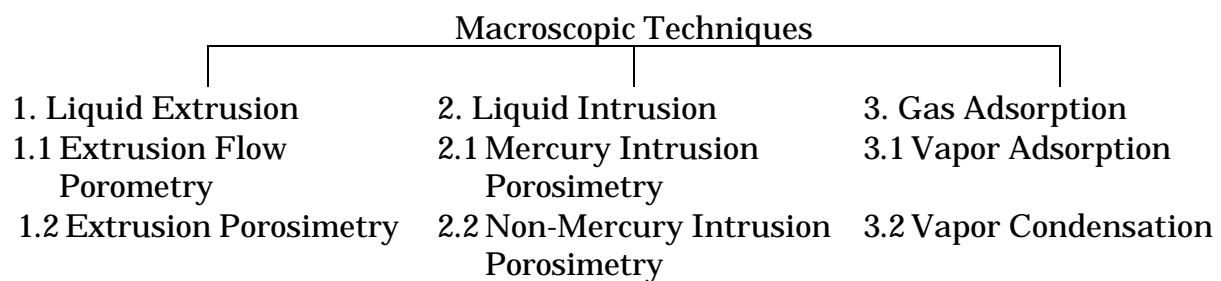


Figure 6. Characterization techniques

5. Extrusion Flow Porometry

5.1 Principle

The liquid whose surface free energy with a solid ($\gamma_{\text{solid/liquid}}$) is less than the surface free energy of the solid with gas ($\gamma_{\text{solid/gas}}$) would wet the solid. Such liquids are known as wetting liquids. A wetting liquid fills the pores spontaneously, but cannot be removed spontaneously. A non-reacting gas can be used to displace liquid from pores and permit gas flow through the pores. For liquid to be displaced [1] (Figure 7):

Work done by gas = Increase in surface free energy

$$p \, dV = (\gamma_{\text{solid/gas}} - \gamma_{\text{solid/liquid}}) \, dS \quad (2)$$

where p is differential pressure, dV is increase in volume of gas in the pore and dS is increase in solid/gas interfacial area and the corresponding decrease in solid/liquid interfacial area.

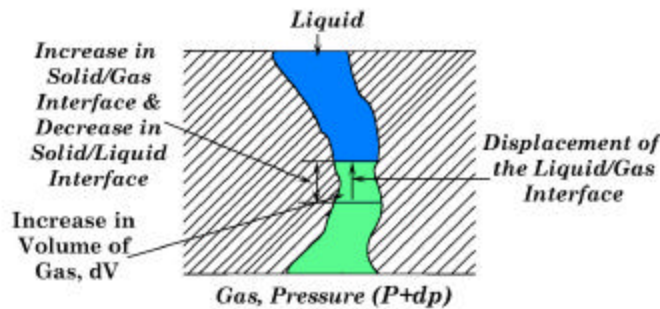


Figure 7. Displacement of wetting liquid in a pore by a gas.

In terms of contact angle [2] (Figure 8):

$$(\gamma_{\text{solid/gas}} - \gamma_{\text{solid/liquid}}) = \gamma \cos \theta \quad (3)$$

where γ and θ are surface tension and contact angle of the wetting liquid.

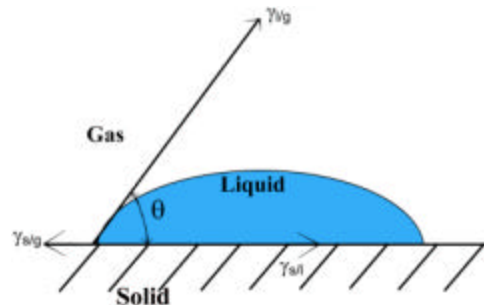


Figure 8. Contact angle of the wetting liquid ($90 \geq \theta \geq 0$).

Substituting in Equation 2 from Equation 1 (definition of pore diameter) and Equation 3:

$$\begin{aligned} p &= \gamma \cos \theta [dS/ dV] \\ &= 4 \gamma \cos \theta / D \end{aligned} \quad (4)$$

For low surface tension wetting liquids contact angle may be taken as zero [3]. This relation shows that the largest pore will be cleared at the lowest pressure and smaller pores will require higher pressures (Figure 9).

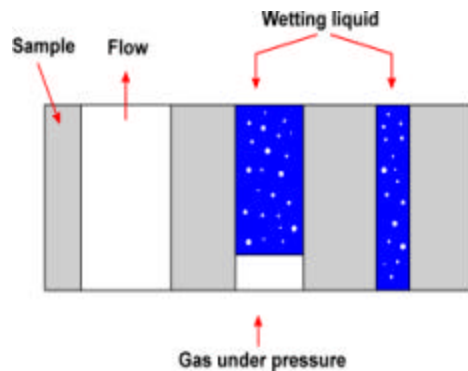


Figure 9. Displacement of wetting liquid from pores.

Differential pressures & flow rates through wet & dry samples are measured. These measured data are used to compute many of the pore characteristics.

5.2 Measurable characteristics

Constricted through pore diameter: The technique detects the presence of a pore when gas flow through the pore is initiated due to complete removal of the liquid from the pore at a certain differential pressure. The differential pressure is used to calculate the pore diameter. Figure 10 shows a through pore with the most constricted part in the middle. Gas pressure required to displace liquid in the pore will increase and will be maximum at the most constricted part. Once this pressure is reached all the liquid from the pore beyond the most constricted part will be removed, gas will flow through the pore and its presence will be detected. Thus, the differential pressure that permits flow through a pore is the differential pressure required to displace liquid at the most constricted part of the pore and the pore diameter calculated from this differential pressure is the diameter of the pore at its most constricted part.

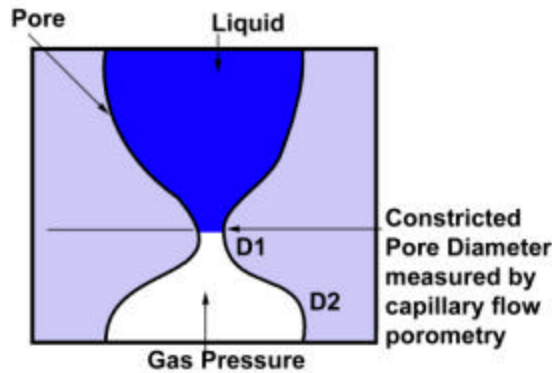


Figure 10. Most constricted pore diameter of through pore

The largest constricted through pore diameter: The largest most constricted through pore diameter corresponds to the pressure at which gas flow begins through wet sample. This is the bubble point pressure (Figure 11). The instrument detects this pressure accurately and computes the bubble point pore diameter. Data in Figure 11 yield a value of 10.237 μm for the bubble point pore diameter of the filtration medium.

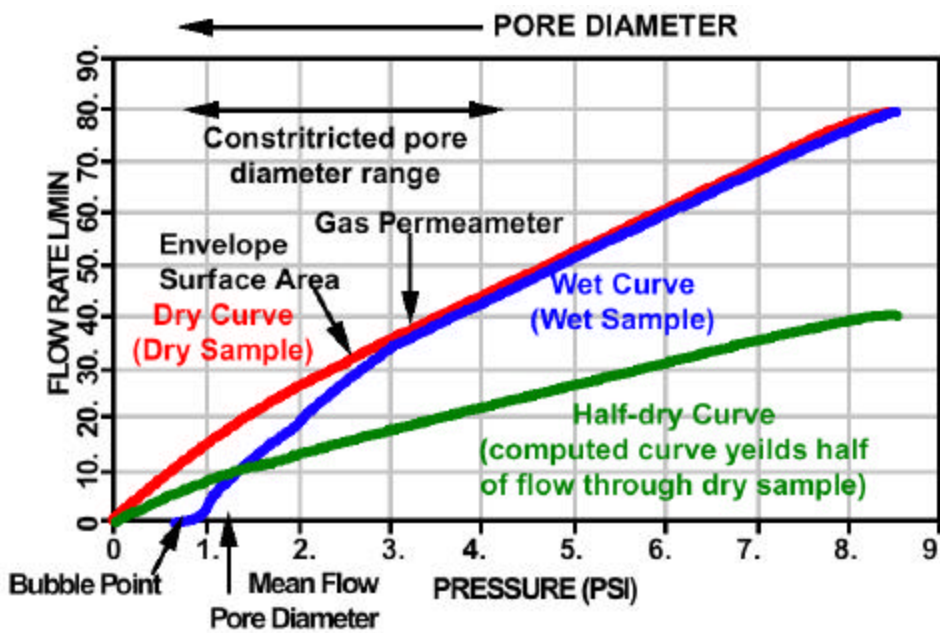


Figure 11. Wet and dry curves obtained using a filtration medium

The constricted mean flow through pore diameter: In order to compute the mean flow pore diameter, the half-dry curve is first computed to yield half of the flow rate through dry curve at a differential pressure. The differential pressure at which the wet curve intersects the half-dry curve is used to compute the mean flow

pore diameter. The mean flow pore diameter is such that half of the flow is through pores larger than the mean flow pore diameter. Mean flow through pore diameter from data in Figure 11 is computed to be 5.038 μm .

The constricted through pore diameter range: The pressure at which the dry and the wet curves meet give the smallest constricted through pore in the filtration material. The bubble point gives the largest constricted pore diameter. The data in Figure 11 yield constricted through pore diameter range of 1.5 – 10 μm .

Pore size and flow distribution: The distribution is given in terms of the distribution function, f:

$$f = - [(d f_w / d d) \times 100 / d D] \quad (5)$$

where f_w is wet flow and f_d is dry flow. The distribution curve is in Figure 12. The area under this curve in any pore size range is the percentage flow in that range.

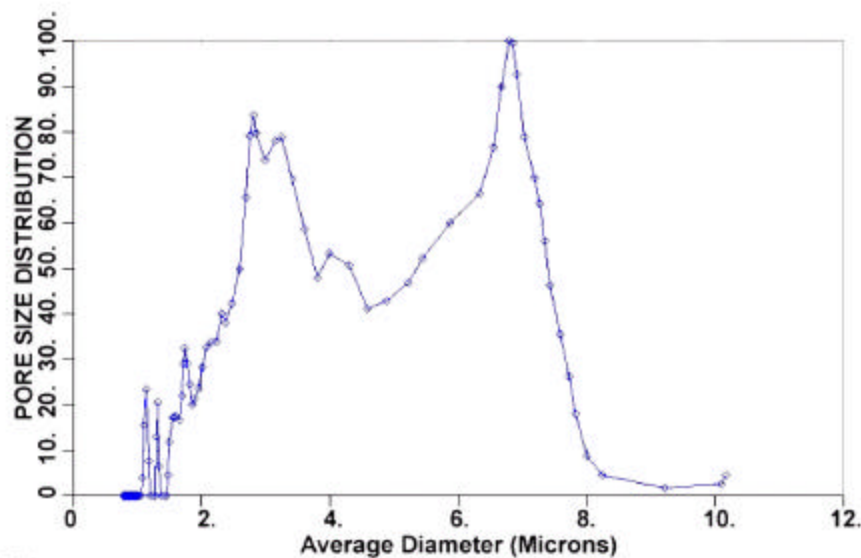


Figure 12. Pore distribution in the filtration medium

Gas permeability: Gas permeability is computed from gas flow rate through the dry sample (Figure 11) using Darcy's law [4]. Permeability may be computed in any desired unit like Darcy, Frazier, Gurly and Rayle at the desired pressure.

$$F = k (A / 2\mu l p_s) (p_i + p_o) [p_i - p_o] \quad (6)$$

F = flow rate in volume at STP

k = permeability

A = cross-sectional area

μ = viscosity of fluid

l = thickness of sample
 p_s = standard pressure
 p_i = inlet pressure
 p_o = outlet pressure

Envelope surface area: Envelope surface area is computed from flow rate through the dry sample (Figure 12) using Kozeny-Carman relation [5].

$$\left[\frac{F l}{p A} \right] = \left\{ \frac{P^3}{[K(1-P)^2 S^2 \mu]} \right\} + \left[\frac{Z P^2 \pi}{(1-P) S (2 \pi \rho p)^{1/2}} \right] \quad (7)$$

F = flow rate in volume at the average pressure
 P = porosity (pore volume / total volume)
 $= [1 - (\rho_b / \rho_a)]$
 ρ_b = bulk density of porous material
 ρ_a = true density of porous material
 S = through pore surface area per unit volume of solid
 ρ = density of the gas at the average pressure
 p = average pressure, $[(p_i + p_o) / 2]$
 K = a constant dependent on the geometry of the pores. It has a value close to 5 for random pored media
 Z = a constant. It is $(48 / 13 \pi)$.

Samples with small surface (Figure 13) area and small concentration of blind pores give results consistent with results determined by gas adsorption (Table 2).

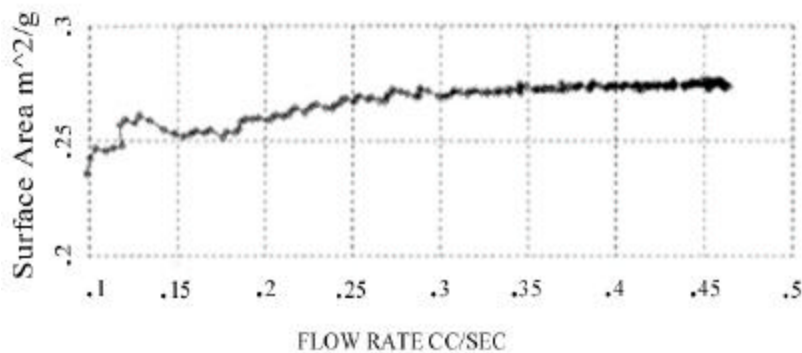


Figure 13. Surface area of a filter material measured as a function of flow rate.

Table 2. Surface area of filtration media measured by two techniques

| Technique | Surface area |
|----------------|------------------------|
| Flow porometry | 0.56 m ² /g |
| Gas adsorption | 0.52 m ² /g |

Liquid permeability: Computed from liquid flow rate (Figure 14) using Darcy's law.

$$F = k (A / \mu l) (p_i - p_o) \quad (8)$$

Typical results are in figure 15. For this material, $k = 8.924 \times 10^{-4}$ darcies

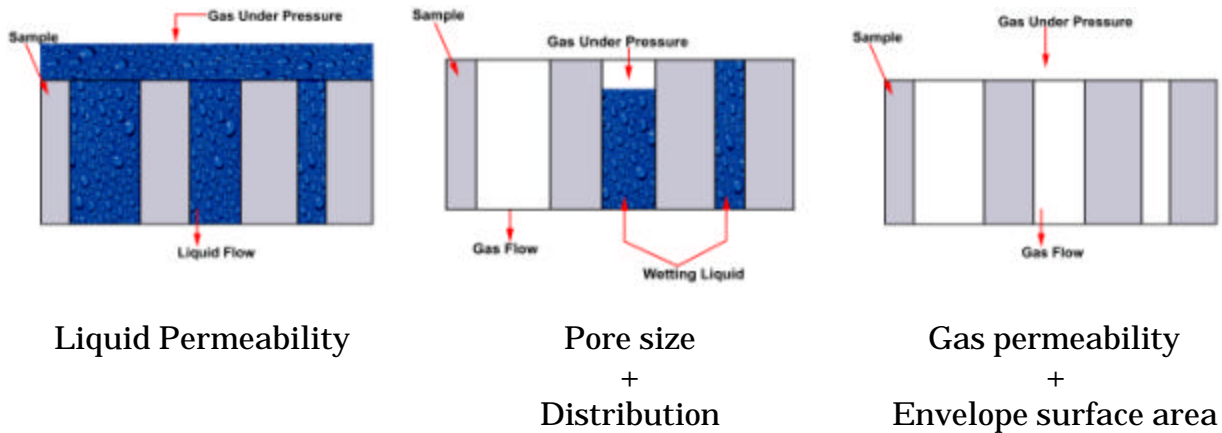


Figure 14. Procedures for measuring different properties by the same technique.

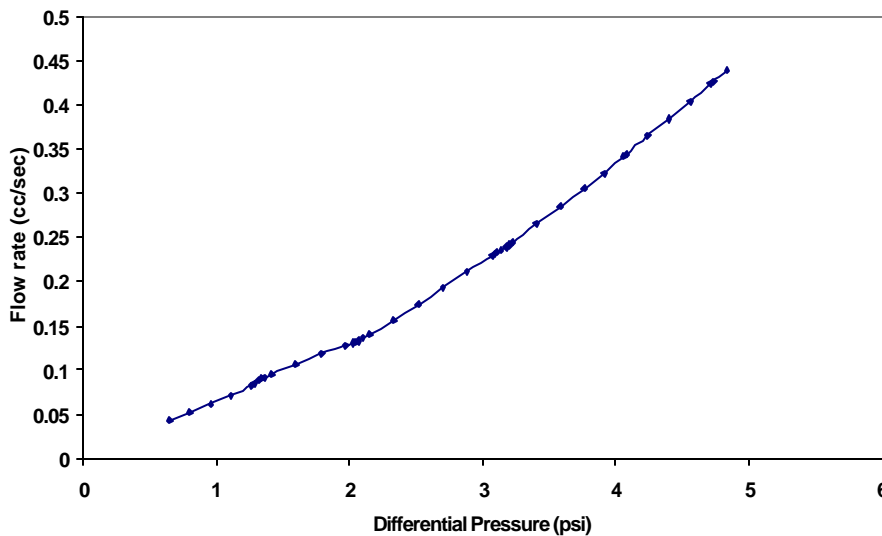


Figure 15. Change of flow rate of water through a filter material as a function of differential pressure.

4.3 Measurement of the effects of service environment

Compressive stress: Filtration media often experience compressive stresses in application. Effect of compressive stress on pore structure can be considerable [6] as demonstrated by data obtained using the porometer (Figure 16).

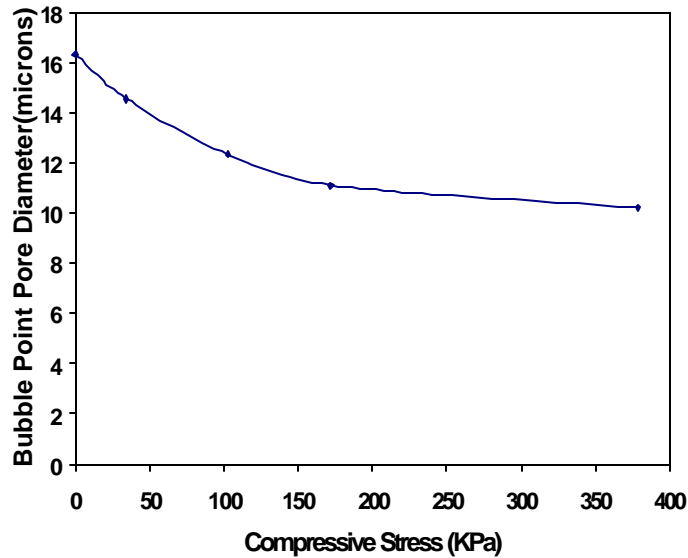


Figure 16. Effect of compressive stress on a battery separator

Cyclic compression: Filtration media are subjected to cyclic stresses during many applications. De-watering in the paper industry is one example. Table 3 shows that the effect can be considerable.

Table 3. Effect of cyclic compression on Pore diameter measured in a cyclic compression porometer.

| Material | Max. comp. stress, psi | No. of cycles | % Change, Bubble point | % Change, Mean flow pore dia. |
|----------|------------------------|---------------|------------------------|-------------------------------|
| Felt #1 | 500 | 15 | - 71.1 | - 30.3 |
| Felt #2 | 750 | 2000 | - 68.4 | - 15.8 |

Strong chemical environment: In many applications filtration media must operate in strong chemical environments. The characteristics in the application environment is relevant. Permeability of 31 % KOH solution measured in the porometer [7] is shown in Figure 17

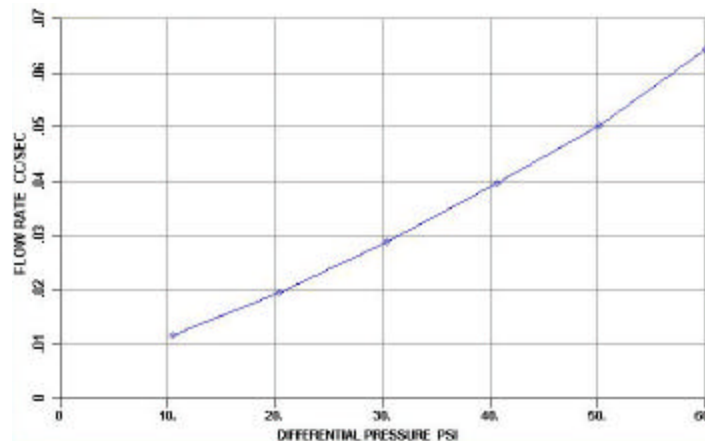


Figure 17. Permeability of 31% KOH solution.

Orientation (x, y & z directions): The pore structure in different directions can be considerably different. This is demonstrated by data (Table 4) generated in an in-plane porometer.

Table 4. In-plane (x - y plane) and through-lane (z direction) pore diameters of different materials

| Material Tested | Material Thickness, mm | Bubble Point Pore Diameter, μm | | Ratio of Pore Diameters |
|---|------------------------|---|----------|-------------------------|
| | | Through-plane | In-plane | |
| Wrapping Paper (thin) | 0.06 | 26.3 | 0.96 | 27.4 |
| Printer Paper | 0.08 | 12.4 | 1.10 | 11.3 |
| Photocopier Paper | 0.08 | 9.08 | 0.73 | 12.4 |
| “Kraft” envelope paper | 0.14 | 15.5 | 1.13 | 13.7 |
| Notepad Backing-Cardboard | 0.92 | 6.70 | 3.53 | 1.90 |
| Transmission Fluid Filter Felt (thick, dense) | 1.90 | 80.4 | 43.3 | 1.86 |
| Meltblown Sheet (dense) | 1.80 | 114.3 | 68.8 | 1.66 |
| Poly Felt Blanket (soft) | 2.00 | 51.8 | 19.8 | 2.62 |
| Poly Filter (hard, thin) | 0.49 | 51.1 | 24.1 | 2.12 |
| Liquid Filter (thick, hard) | 1.50 | 34.5 | 15.3 | 2.25 |

Temperature: Properties of filtration material can vary considerably with change in application temperature. Porometers have the ability to measure permeability up to 200° C and pore structure up to 100° C. An example is shown in Figure 18.

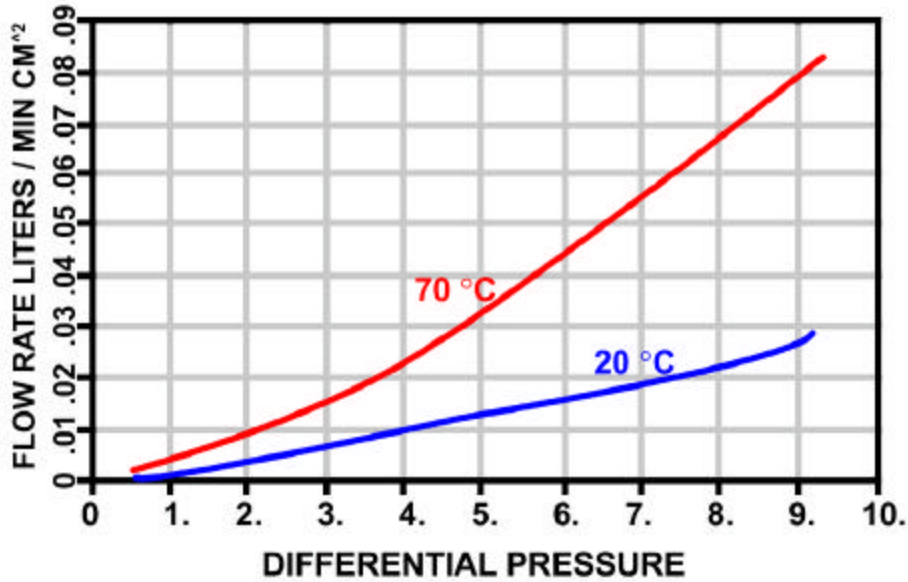


Figure 18. Gas permeability at two temperatures. Red 70 °C. Blue 20 °C

Layered structure: Multilayered, graded and coated filtration media are widely used. The porometer can measure pore structure of each layer in-situ without separating the layers [9,10]. The pore distributions in the two layers of a hot gas filtration media are shown in Figure 19.

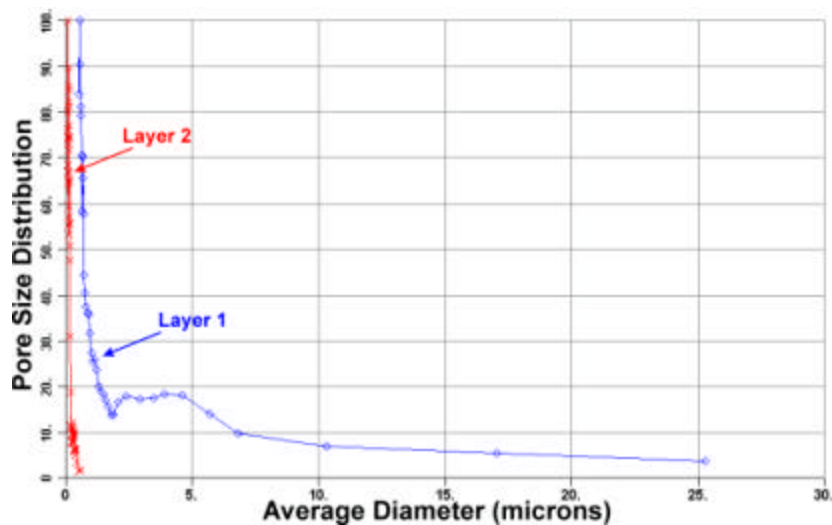
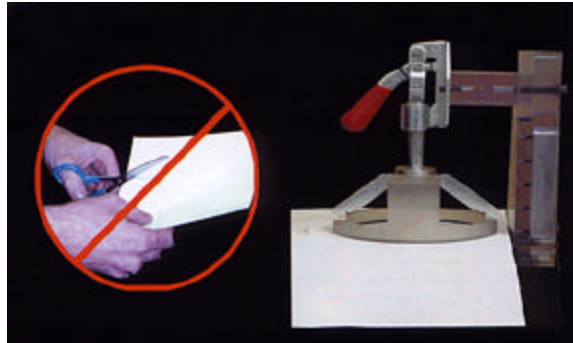


Figure 19. Pore distribution of each layer of a two-layer hot gas filter determined in-situ.

Testing without cutting or damaging filtration media: It is often required to test bulk filtration media at many locations without damaging the bulk material in

any way. The mobile sample chamber of a porometer can be clamped on to the test area or the bulk material could slide through the sample chamber (Figure 20).



(a)



(b)

Figure 20. Sample chambers for testing without damaging the filtration media. (a) Sample chamber that clamps on the bulk material. (b) Sample chamber that permits the bulk material to slide through.

5.4 Instrument

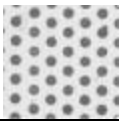
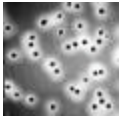
Technology: In the porometer, test execution, data acquisition, data storage and data reduction are often fully automated. Windows based operation of the instrument is simple. In this study, the PMI Capillary Flow Porometer was used (Figure 21).



Figure 21. The Capillary Flow Porometer used in this investigation.

Accuracy: The accuracy of data obtainable with a porometer is demonstrated by the results shown in Table 5.

Table 5. Pore diameters measured by SEM and porometer

| Sample | SEM Micrograph | Pore diameter, μm | |
|-----------------------------|---|------------------------------|----------------|
| | | SEM | PMI Porometer |
| Etched stainless steel disc |  | 81.7 ± 5.2 | 86.7 ± 4.1 |
| Polycarbonate membrane |  | 4.5 ± 0.5 | 4.6 ± 0.1 |

Repeatability: Repeatability of results obtainable with a porometer is demonstrated by data in Table 6 [3].

Table 6. Percentage scatter in 32 measurements of bubble point pressure

| Filter | Wetting Liquid | |
|--------------------------|----------------|---------|
| | Porewick | Silwick |
| Sintered Stainless Steel | 1.8% | 1.2% |
| Battery Separator | 0.2% | 1.5% |
| Paper | 1.7% | 1.1% |

6. Extrusion Porosimetry

6.1 Principle

The sample is placed on a membrane such that its largest pore is smaller than the smallest pore of interest in the sample. Pores of the sample and the membrane are filled with a wetting liquid.

Pressure of a non-reacting gas on the sample is increased on the sample. Pressurized gas displaces liquid from pores. The pressure required to displace the wetting liquid is given by Equation 4, which suggests that higher pressure is required to remove liquid from smaller pores. Applied pressure is sufficient to remove liquid from pores of the sample, but not high enough to remove liquid from pores of the membrane. Displaced liquid from pores of the sample passes through the liquid filled pores of the membrane and is measured, while the liquid filled

pores of the membrane prevent the gas to pass through (Figure 22). The pressure is used to compute pore diameter [11,12,13].

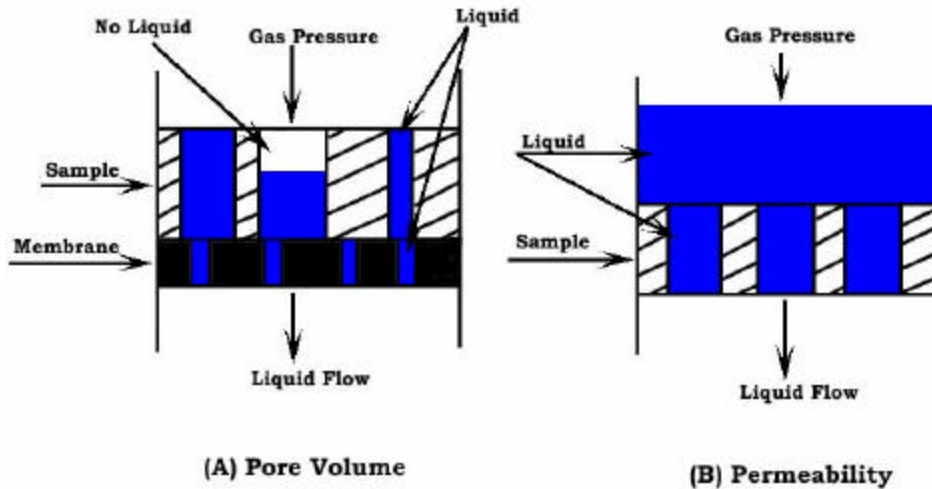


Figure 22. Principle of extrusion porosimetry

For measurement of liquid permeability, volume of displaced liquid due to pressure on excess liquid on the sample is measured. The membrane is removed if resistance of the membrane to flow is appreciable compared with that of the sample. (Figure 22).

6.2 Measurable characteristics

Multiple diameters of through pores: In this technique only through pores are measured. Consider the pore in Figure 23. With increase in pressure the liquid is displaced from the pore until the most constricted part of the pore. At this point the pressure is the highest and all the liquid beyond the most constricted part of the pore is removed. Thus all pore diameters of the pore from the entry point of the gas to the most constricted part of the pore are measured. However, the pore volume associated with the most constricted pore diameter is the volume of the pore beyond the most constricted part. Thus for wide mouth pores the volume of the most constricted part of the pore is over estimated.

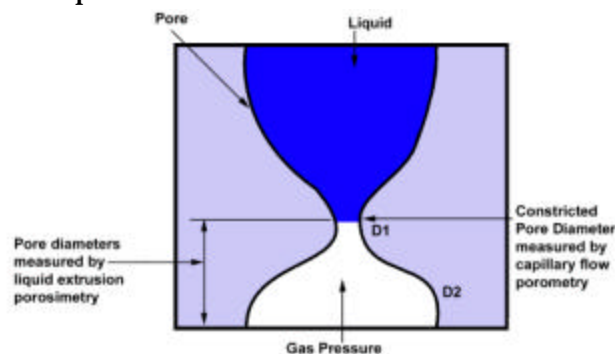


Figure 23. Pore diameters of a pore measured by extrusion porosimetry

Through pore volume & diameter: Through pore volume of a filtration medium measured by extrusion porosimetry is shown in Figure 24 along with the pore diameter. The pore volume is 0.421 cm³/g. The porosity is 67.12 %.

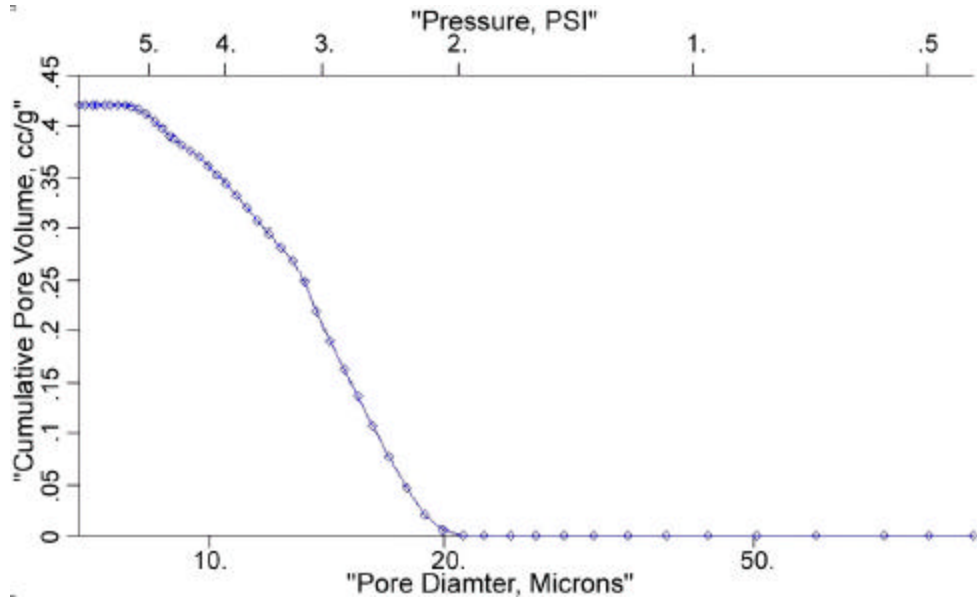


Figure 24. Through pore volume of hydrogel

Through pore volume distribution and median pore diameter: The volume distribution is given by the distribution function:

$$f_v = - (dV/d \log D) \tag{9}$$

where V is pore volume and D is pore diameter. The function is such that the area under the distribution function in any pore diameter range yields the volume of pores in that range. Pores as large as 2000 μm are measurable. Pores having appreciable pore volume are in the range of 50 to 2000 μm (Figure 25).

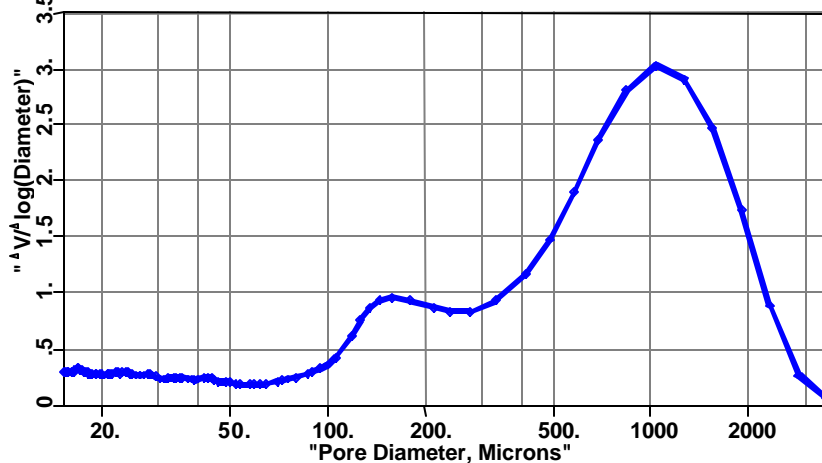


Figure 25. Volume distribution in ceramic foam

Through pore surface area: Through pore surface area is computed from pore volume measured as a function of pressure using the following equation derived from Equations 2 & 3. The through pore surface area of a ceramic filter measured by extrusion porosimetry was 0.52 m²/g

$$S = [1/(\gamma \cos \theta)] \int p \, dV \quad (10)$$

Liquid permeability: Liquid permeability is computed from liquid flow rate using the following equation based on Darcy's law. The permeability of water computed from water flow rate through a depth filtration medium (Figure 26) using Equation 8 is 6.5 Darcies.

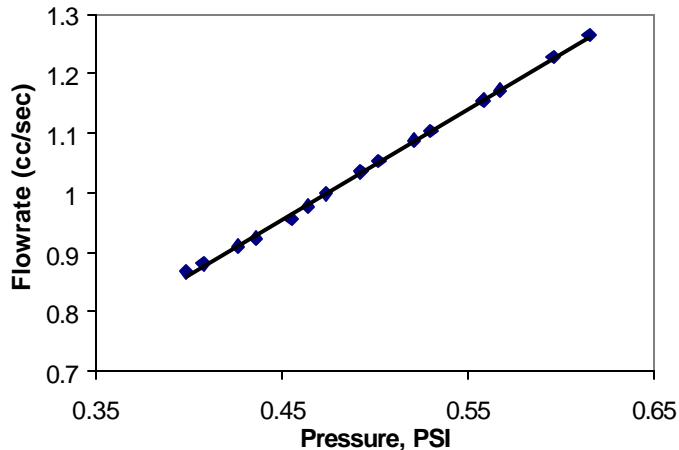


Figure 26. Water flow rate through a depth filtration medium measured by extrusion porosimetry.

6.3 Instrument

Extrusion porosimeters are fully automated instruments. They are capable of using many wetting liquids, require low pressures to operate and no toxic material is used. Tests can be performed under a variety of simulated service conditions. The PMI Liquid Extrusion Porosimeter used in this study is shown in Figure 27.



Figure 27. Liquid Extrusion Porosimeter used in this study

7. Mercury Intrusion Porosimetry

7.1 Principle

Mercury is non-wetting for most materials. For a non-wetting liquid, ($\gamma_{\text{solid/gas}} < \gamma_{\text{solid/liquid}}$) and contact angle, $\theta > 90$. Therefore, mercury surrounding a non-wetting material cannot spontaneously flow into its pores. Mercury can be forced into pores by applying pressure. Equating the work done due to forcing mercury into a pore to the increase in surface free energy and using the definition of pore diameter:

$$p = - 4\gamma \cos \theta / D \quad (11)$$

Measured differential pressure yields pore diameter and volume of intruded mercury gives pore volume (Figure 28).

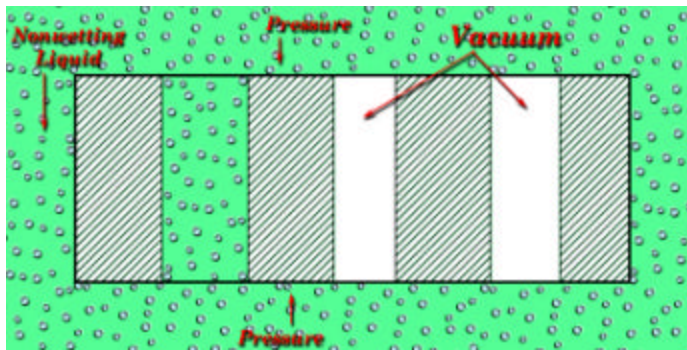


Figure 28. Principle of mercury intrusion porosimetry

7.2 Measurable characteristics

Multiple diameters for a through or blind pore: In this technique, as mercury at a given pressure intrudes a certain part of a pore the diameter of that part of the pore is obtained from pressure. Thus, multiple diameters for each through and blind pore are measured (Figure 29).

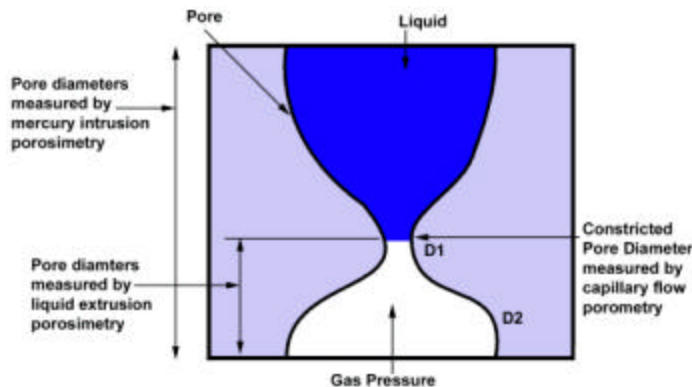


Figure 29. Multiple diameters detected for each pore.

Volume and diameter of through & blind pores: Increase in pore volume with an increase in pressure (decrease in pore diameter) is normally measured (Figure 30)

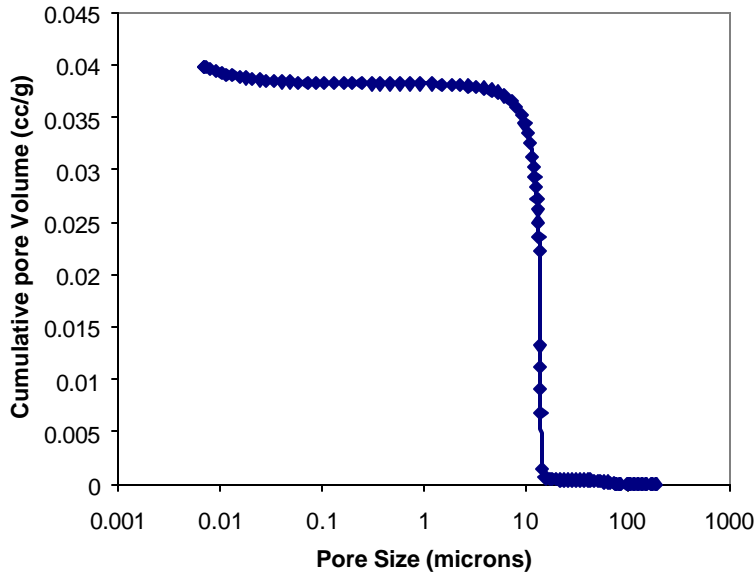


Figure 30. Pore volume of depth filtration medium as a function of (pore diameter) measured by mercury intrusion porosimetry.

Through & blind pore volume distribution: The pore volume distribution is given by the distribution function, f_v defined in Equation 9. The distributions by mercury intrusion and liquid extrusion agree very well with each other in case of the depth filtration media (Figure 31).

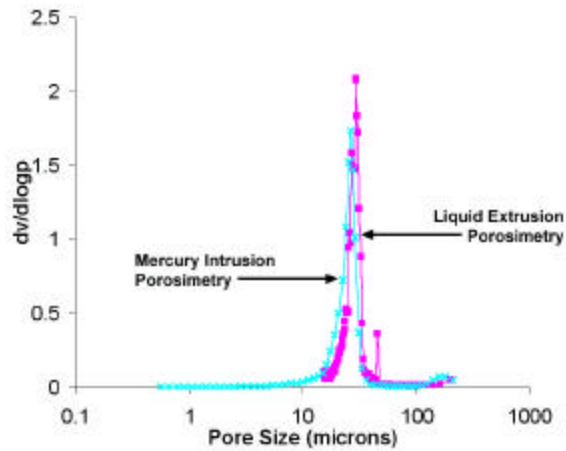


Figure 31. Pore volume distribution in depth filtration medium

Surface area (total) of through & blind pores: The surface area is computed from the variation of volume with pressure using the following relation.

$$S = [1/(-\gamma \cos \theta)] \int p dV \quad (12)$$

7.3 Instrument

Mercury intrusion porosimeters are available in which test execution, data acquisition, data storage, mercury refill, cleaning and data reduction are fully automated. Windows based operation is simple. Instruments are available in many designs. Designs with minimal contact with mercury are also available.

8. Non-Mercury Intrusion Porosimetry

Non-mercury intrusion porosimetry works just like a mercury intrusion porosimeter except that the design permits use of a non-mercury non-wetting liquid as the intrusion liquid. Liquids like water, oil and any other non-wetting application liquid can be used. The data obtained are similar in both techniques (Figure 32).

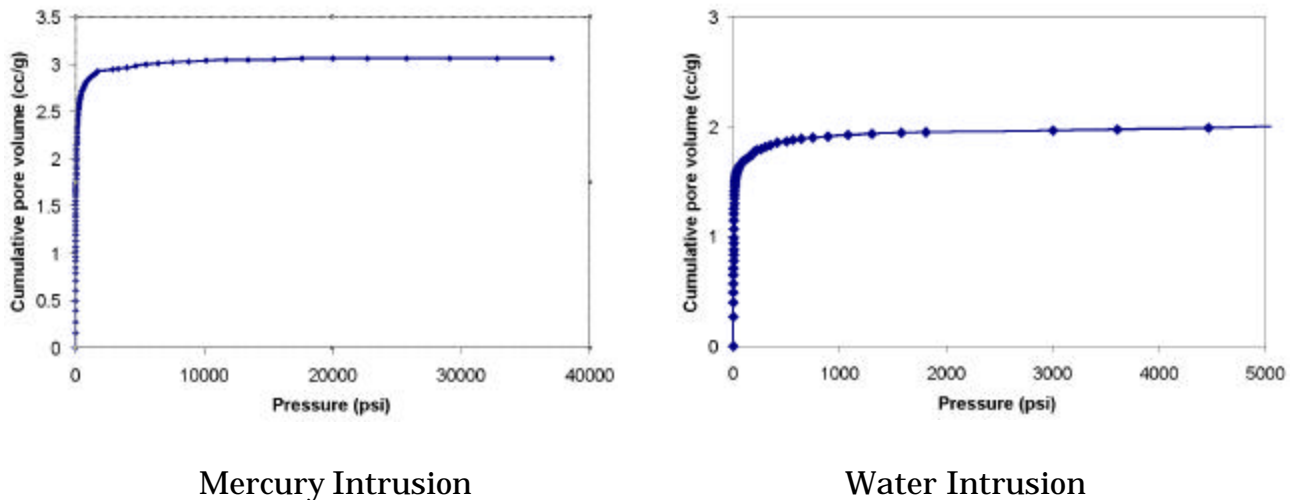


Figure 32. Change of intrusion volume with pressure.

This technique has a number of advantages over mercury intrusion porosimetry. In this technique no toxic material is used. Pressures required are almost an order of magnitude less. Use of application liquid creates the application environment.

9. Vapor Adsorption Technique

9.1 Principle

A clean surface adsorbs gases and vapors. The amount of vapor adsorbed on the pore surface is measured as a function of pressure of the vapor below its equilibrium pressure. The following equation based on the BET theory relates vapor

pressure and amount of the adsorbed gas to the amount of the gas required to form a monolayer [14].

$$\frac{p}{(p_0 - p)W} = \frac{1}{W_m C} + \frac{(C-1)}{W_m C} \left(\frac{p}{p_0}\right) \quad (13)$$

where:

p = vapor pressure

p_0 = equilibrium vapor pressure

W = amount of adsorbed gas

C = a constant

W_m = amount of gas required to form a monolayer

At low vapor pressures [$0.05 \leq (p/p_0) \leq 0.35$], the plot of $[p/(p_0 - p)W]$ against (p/p_0) is usually linear. The slope and intercept of this straight line yields W_m . The surface area is computed from W_m using the following relation.

$$S = W_m N \alpha / m \quad (14)$$

where:

S = surface area per unit mass

W_m = amount of gas to form a monolayer in moles

N = Avogadro's number

α = cross-sectional area of the adsorbed vapor molecule

m = mass of sample

9.2 Measurable characteristic

Figure 33 shows a typical linear plot that one obtains when adsorption data are plotted after BET theory. Surface area is computed from such plots. This technique is considered to be the most accurate technique for determining surface area of samples with large specific surface area. Surface area of filtration media measured using vapor adsorption technique and flow porometry usually agree very well with each other (Table 2).

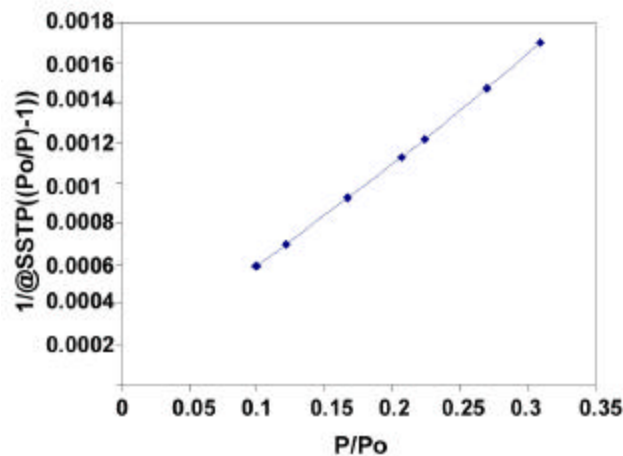


Figure 33. Linear behavior of adsorption data plotted after BET theory.

9.3 Instruments

The tests are normally performed at liquid nitrogen temperature. There are many instrument designs available. Some of the designs are very simple and are capable of generating repeatable data rapidly. Sophisticated designs can be slow, but the results are more accurate. Figure 34 shows a compact instrument capable of rapid generation of data.



Figure 34. QBET capable of quick test.

10. Vapor Condensation Technique

10.1 Principle

If the liquid/pore surface free energy is less than the vapor/pore surface free energy, liquid contained in a pore will have less free energy than bulk liquid. Vapor at equilibrium vapor pressure can condense to form bulk liquid. Therefore, vapor at pressures below the equilibrium vapor pressure can condense in small pores (Figure 35). Condensation occurs in smallest pore at the lowest vapor pressure and as the vapor pressure approaches equilibrium vapor pressure condensation occurs in the larger pores.

Pore diameter is related to vapor pressure. Let liquid, l of volume dV condense in a pore from vapor, $v(p)$ at pressure, p and the resulting conversion of the solid/vapor surface area in to solid/liquid surface area be dS (Figure 35). For condensation of liquid of molar volume \underline{V} :

$$(dV / \underline{V}) \Delta G [v(p) \rightarrow l (\text{bulk})] + dS \Delta G [s/v \rightarrow s/l] = 0$$

We know that in terms of equilibrium vapor pressure, p_0 , of the liquid:

$$\Delta G [v(p) \rightarrow l (\text{bulk})] = \Delta G [v(p) \rightarrow v(p_0)] = RT \ln (p_0 / p)$$

$$\Delta G [s/v \rightarrow s/l] = (\gamma_{s/l} - \gamma_{s/v}) = - \gamma \cos \theta$$

From these relations and the definition of pore diameter:

$$\ln (p/p_0) = - [4 \underline{V} \gamma \cos \theta / RT] / D \tag{15}$$

where R is the gas constant and T is the absolute temperature

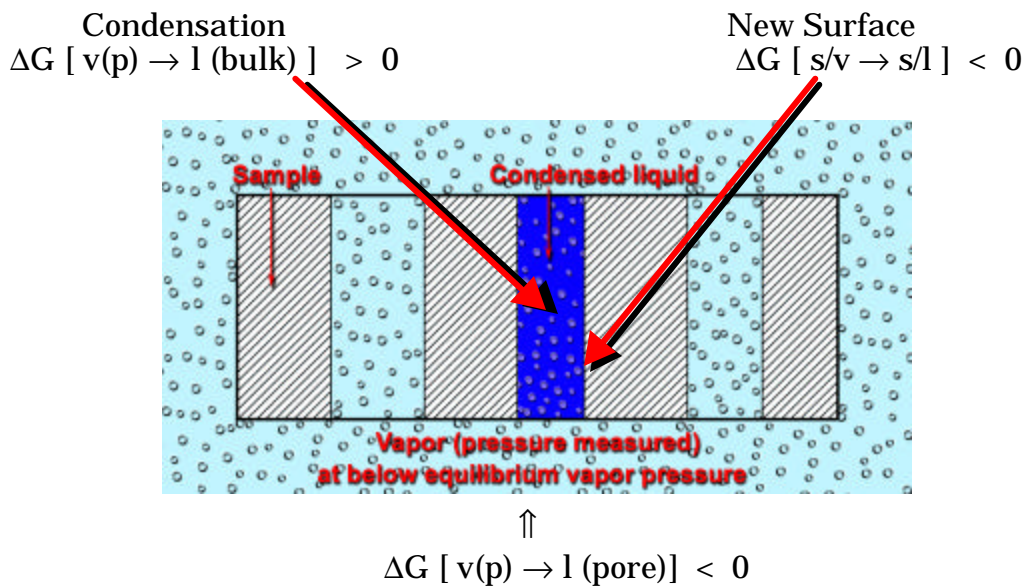


Figure 35. Condensation in pores.

10.2 Measurable characteristics

Multiple diameters of through & blind pores: When liquid condenses in a certain part of the pore at a certain pressure of the vapor, the diameter of that part of the pore is measured. Thus, multiple diameters of each through and blind pore are measured (Figure 36).

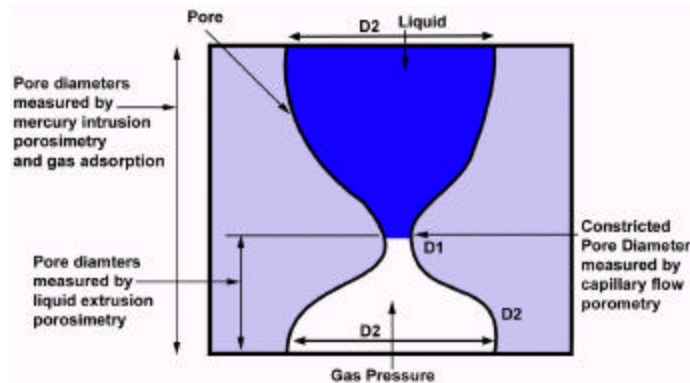


Figure 36. Multiple diameters of pores measurable

Volume and pore diameter of through & blind pores: Figure 37 is a plot of pore volume measured as a function of pore diameter. The measurable pore diameters are usually between 1-0.0005 μm .

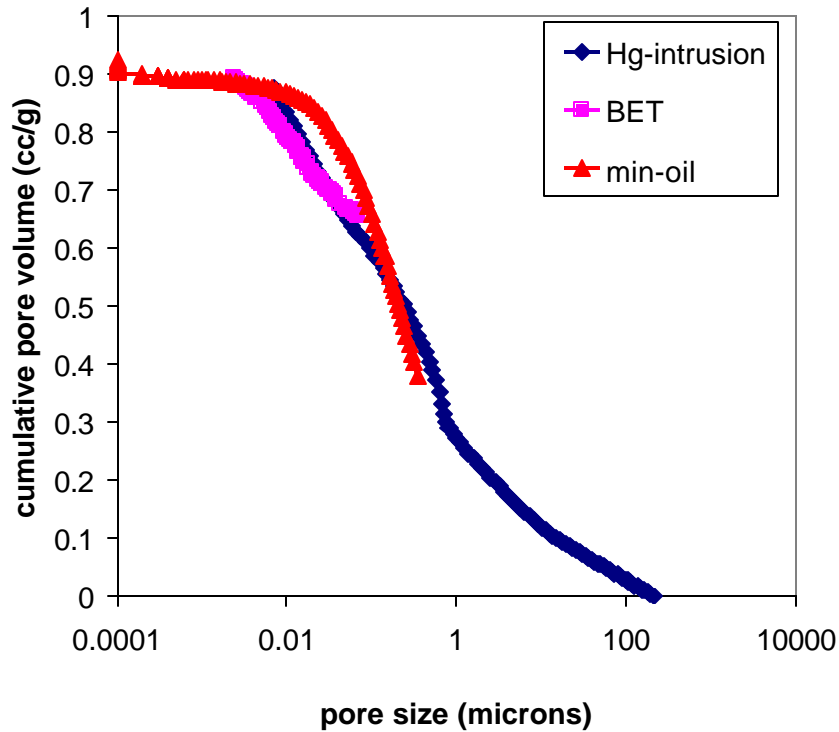


Figure 37. Pore volume and diameter measured by vapor condensation. Pore volumes measured by mercury intrusion porosimetry and non-mercury (oil) intrusion porosimetry are also shown for comparison.

Through & blind pore volume distribution: The pore distribution is given in terms of the distribution function. Defined in Equation 9. One example is shown in Figure 38.

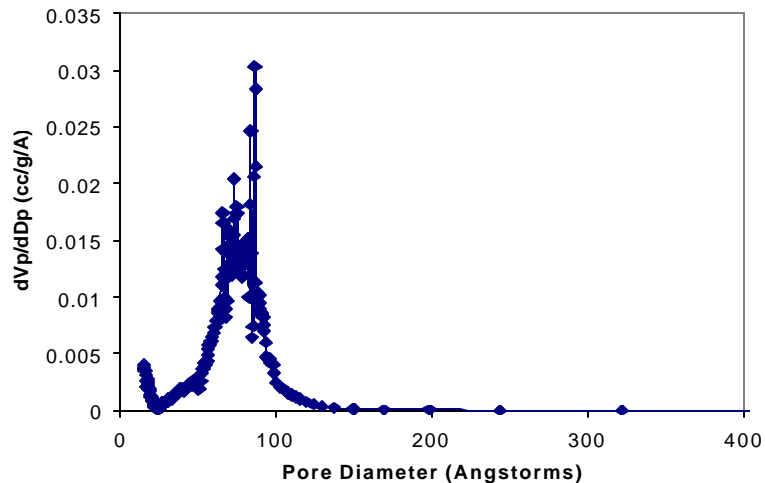


Figure 38. Pore distribution measured by vapor condensation.

10.3 Instrument

These instruments are usually very sophisticated and fully automated. The surface area, pore volume, pore diameter and pore distribution can be measured in the same instrument. These instruments also have the ability to measure chemisorption of chemicals, and adsorption and desorption isotherms. Many designs are commercially available.

11. Capabilities of the Techniques

Many applications of these techniques and their relative strengths have been documented [15,16]. The capabilities of the techniques, their strengths and limitations have been summarized in Tables 7, 8 and 9.

Table 7. Capabilities of the techniques

| Capability | Extrusion flow porometry | Extrusion porosimetry | Intrusion porosimetry (mercury) | Intrusion porosimetry (non-mercury) | Gas adsorption |
|-------------------------------------|---|-----------------------|---------------------------------|-------------------------------------|----------------|
| | Through pore diameter | | | | |
| The most constricted | √ | × | × | × | × |
| The largest of the most constricted | √ | × | × | × | × |
| Many diameters of a pore | × | √ | √ | √ | √ |
| Diameter range, μm | 500-0.013 | 2000-0.05 | 300 -0.03 | 20-0.001 | 1-0.0005 |
| | Through pore volume | | | | |
| Volume | × | √ | × | × | × |
| | Through pore surface area | | | | |
| Surface area | √ | √ | × | × | × |
| | Permeability | | | | |
| Liquid | √ | √ | × | × | × |
| Gas | √ | × | × | × | × |
| | Through & Blind Pores | | | | |
| All diameters | × | × | √ | √ | √ |
| Volume | × | × | √ | √ | √ |
| Surface area | × | × | √ | √ | √ |
| | Testing under simulated service conditions | | | | |
| Many properties | √ | √ | × | × | × |

Table 8. Operational features.

| Capability | Extrusion flow porometry | Extrusion porosimetry | Intrusion prosimetry (mercury) | Intrusion porosimetry (non-mercury) | Gas adsorption |
|---------------------------|--------------------------|-----------------------|--------------------------------|-------------------------------------|----------------|
| Use of toxic material | × | × | √ | × | × |
| High pressure | × | × | √ | × | × |
| Subzero temperature | × | × | × | × | √ |
| Use of fluid of interest | √ | √ | × | √ | × |
| Involved / time consuming | × | √ | √ | × | √ |

Table 9. Strengths and limitations of techniques

| Strengths | Limitations |
|---|---|
| Extrusion Flow Porometry | |
| 1. Versatile. | 1. Pore volume not measurable |
| Measures a wide variety of through pore characteristics: | 2. Blind pores not measurable |
| Constricted pore diameter (Largest, Mean & Range) | 3. $500 > \text{Pore diameter} > 0.013 \mu\text{m}$ |
| Distribution | |
| Gas permeability | |
| Liquid permeability | |
| Surface area | |
| 2. Capable of measuring effects of application environments on pore structure characteristics | |
| 3. Toxic material and high pressure not used | |
| 4. Short test duration | |
| Extrusion Porosimetry | |
| 1. Through pore volume, diameter, Distribution & surface area, and Liquid permeability measurable | 1. Blind pores not measurable |
| | 2. Constricted pore diameter not measurable |

| | |
|--|---|
| 2. Very large pores measurable | 3. Gas permeability not measurable |
| 3. Toxic material & high pressure not Used | 4. Largest pore diameter not measurable |
| 4. Capable of measuring effects of application environment | 5. 2000 >Pore diameter > 0.05 μm |
| Mercury Intrusion Porosimetry | |
| 1. Through & blind pore volume, diameter, distribution & surface area Measurable | 1. Cannot measure permeability 2. Cannot measure largest pore Diameter |
| 2. Usable for a wide variety of materials | 3. Cannot measure constricted pore Diameter |
| | 4. Uses toxic mercury & high pressures |
| | 5. 300 >Pore diameter > 0.03 μm |
| Non-Mercury Intrusion Porosimetry | |
| 1. Through & blind pore volume, diameter, distribution & surface area Measurable | 1. Need to find a non-mercury non-Wetting liquid |
| 2. Toxic materials and high pressures not used | 2. Constricted pore diameter not Measurable |
| 3. Many application fluids usable | 3. Largest pore diameter not measurable |
| | 4. Permeability not measurable |
| | 5. 20 >Pore diameter > 0.001 μm |
| Vapor Adsorption/Condensation | |
| 1. Through & blind pore volume, diameter, distribution & surface area Measurable | 1. Constricted pore diameter not Measurable. |
| 2. Very small pores measurable | 2. Largest pore not measurable |
| 3. No toxic material used | 3. Permeability not measurable |
| | 4. Low temperatures required |
| | 5. 1 > Pore diameter > 0.0005 μm |

12. Examples of Applications

12.1 Homogeneity of filtration media

Manufacturing process often introduces defects in filter material in certain areas. Cutting many samples to test for homogeneity can damage & destroy the filtration media. On-Line Porometer is ideal for such applications. It simply clamps on to the area to be tested or allows the filter material to slide through (Figure 20).

A filtration medium was tested for homogeneity on three areas along its length [17] (Figure 39). In each area, bubble point, mean flow pore diameter and distribution peak position were homogeneous. However, the three areas had considerably different characteristics (Figure 40).



Figure 39. The three areas that were tested.

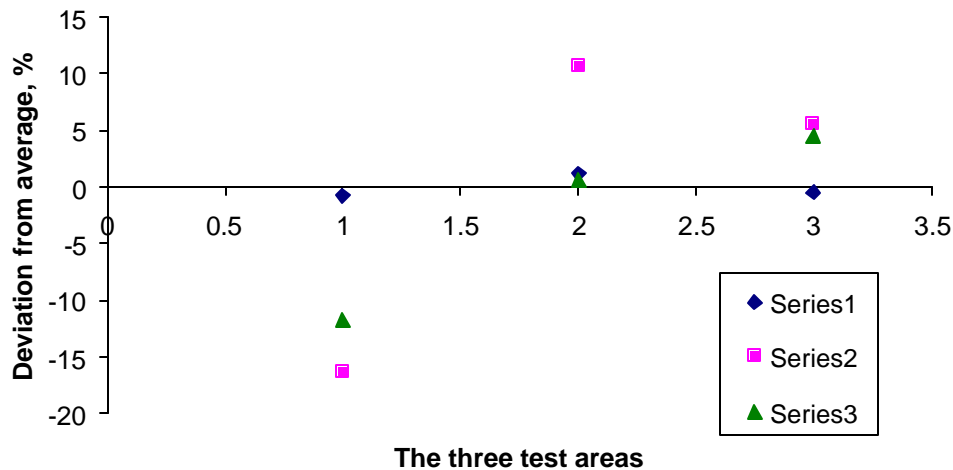


Figure 40. Deviation of pore diameters from the average at three different areas. Bubble point pore diameter (series 1), mean flow pore diameter (series 2) and peak diameter of the distribution peak (series 3) are included in the figure.

Bubble point at the three locations were identical. There was very little deviation from the average value. Deviations of mean flow pore diameter from the average were considerably different; 16.3 % for Area # 1, 10.7 % for Area # 2 and 5.5 % for Area # 3. Position of the pore distribution peak showed similar scatter. The properties of Area # 1 were less than the average, those of Area # 2 were greater than the average and properties of area # 3 were close to the average.

12.2 Design of composite filtration media

Filtration media are required to have suitable pore size, pore size distribution, pore volume, pore surface area and permeability for performing satisfactorily in applications. All desired properties may not be encountered in a filtration medium. Composite filtration media prepared by a suitable combination of filtration material can have the required characteristics. As an illustration we will consider design of composites using six filtration media [18].

Bubble point pore diameter: Bubble points of composite filters, C#1, C#2, C#3 and C#4, containing filter materials 1,2,3,4,5 & 6 are listed in Table 10. The bubble point pore diameter is considerably reduced in all cases. The reduction is as much as 30 to 70 %.

Table 10. Bubble point pore diameters of composite filters

| Filters | Bubble point pore diameter, μm | Deviation from the average value |
|-------------------|---|----------------------------------|
| C#1 (1,6) | 73.53 | - 32 % |
| C#2 (1,2) | 23.09 | - 68 % |
| C#3 (1,2,5) | 21.72 | - 69 % |
| C#4 (1,2,3,4,5,6) | 22.82 | - 67 % |

Mean flow pore diameter: Table 11 lists the mean flow pore diameters of composite filters. The mean flow pore diameter is also considerably reduced in all cases.

Table 11. Mean flow pore diameters of composites

| Filters | Mean flow pore diameter, μm | Deviation from the average value |
|-------------------|--|----------------------------------|
| C#1 (1,6) | 35.00 | - 18 % |
| C#2 (1,2) | 10.38 | - 66 % |
| C#3 (1,2,5) | 9.21 | - 63 % |
| C#4 (1,2,3,4,5,6) | 7.62 | - 74 % |

Structural homogeneity: The scatters (Table 12) in bubble point pore diameter and mean flow pore diameter determined on samples taken from various parts of the composite filter demonstrate that the composites are much more homogeneous than their constituents

Table 12 Scatter in bubble point and mean flow pore diameters of composites.

| Composite | % Scatter in pore diameter | | | |
|-------------|----------------------------|-----------------|-----------|---------------|
| | Bubble point | | Mean flow | |
| | Composite | Constituents | Composite | Constituents |
| C#1(1,6) | 5.5 | 20.8, 9.2 | 3.2 | 4.8, 3.8 |
| C#3 (1,2,5) | 8.3 | 20.8, 6.1, 15.6 | 4.2 | 4.8, 9.4, 7.3 |

| | | | | |
|----------------------|------|----------------|-----|----------------|
| C#4 (1,2,3,4,5,6) | 11.8 | 20.8, 6.1, 5.8 | 3.9 | 4.8, 9.4, 6.3, |
| | | 3.2, 15.6, 9.2 | | 6.4, 7.3, 3.8 |

Effect of number of layers: The bubble point and mean flow pore diameters shown in Tables 10 and 11 suggest that an increasing number of layers do not have corresponding effect on the pore diameter. The pore diameter of a composite consisting of one filter material with large pores and another with small pores can be reduced by adding more filter materials to the composite, but the percentage reduction in the pore diameter can not be increased appreciably. Increasing the numbers of layers does not have a proportional effect on reducing pore diameters.

Thus, the bubble point pore diameter and the mean flow pore diameter could be reduced as much as 70 % in composites. After the large initial reduction, the magnitude of reduction was insensitive to the number of constituent filter materials in the composite. The composite filters were structurally much more homogeneous than the constituents.

12.3 Pore structure of ceramic filtration medium

No one technique can yield all pore structure characteristics of a material. The use of multiple techniques gives much more information about pore structure [16]. The investigation of a ceramic filtration medium using three technique is an example. The results obtained using three techniques is given in Table 13. The pore structure characteristics of the filtration medium are listed in Table 14. A sketch illustrating the expected pore structure in shown in Figure 41.

Table 13. Results obtained using three techniques

| Technique | Measured characteristics |
|---------------------------------|---|
| Extrusion Porosimetry | Volume of through pores: 1.982 cm ³ /g Volume distribution of through pores Many pore diameters of through pores Surface area of through pores: 0.43 m ² /g. |
| Intrusion Porosimetry (Mercury) | Volume of through & blind pores: 2.492 cm ³ /g Volume distribution of through & blind pores All pore diameters of through & blind pores Surface area of through and blind pores: 9.44 m ² /g |
| Extrusion Flow Porometry | Largest constricted through pore diameter: 450.4 μm Mean flow constricted through pore diameter: 3.867 μm. Constricted through pore diameter range: 450.4 - 0.39 μm Flow distribution |

Table 14. Pore structure characteristics of the filtration medium

| | |
|---------------------------------------|---|
| Through pores | |
| The constricted largest pore diameter | 450.4 μm |
| The average constricted pore diameter | 3.867 μm |
| Constricted pore diameter range | 450.4 - 0.39 μm |
| Average of all pore diameters | 18 μm |
| Volume | 1.982 cm^3/g |
| Percent of total pore volume | 79.5 % |
| Surface area | 0.43 m^2/g |
| Percent of total surface area | 5 % |
| Shape | Pores with 4 μm constrictions and >18 μm mouths |
| Blind Pores | |
| Diameter of wide parts | > 18 μm |
| Diameter of narrow parts | \approx 0.02 μm |
| Volume | 0.51 cm^3/g |
| Percentage of total pore volume | 20.5 % |
| Surface area | 9.01 m^2/g |
| Percent of total surface area | 95 % |
| Shape | Wide mouth with long narrow tails |

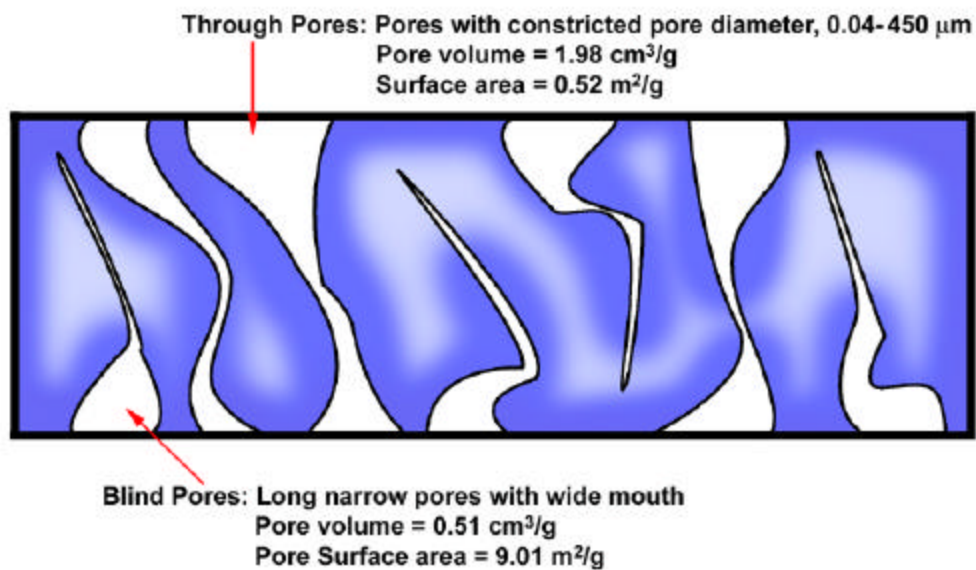


Figure 41. Expected pore structure of ceramic filtration medium.

13. Summary and Conclusions

1. The principles of the following six techniques and the characteristics measurable by these techniques have been discussed.
 - Extrusion Flow Porometry
 - Extrusion Porosimetry
 - Mercury Intrusion Porosimetry
 - Non-Mercury Intrusion Porosimetry
 - Vapor Adsorption Technique
 - Vapor Condensation Technique
2. Experimental data have been presented to illustrate the measurement of pore structure characteristics.
3. Significance of measured characteristics has been discussed.
4. Relative strengths and weaknesses of all the techniques have been discussed.
5. Examples of applications for design have been included.

14. References

1. Akshaya K Jena and Krishna M Gupta, In-plane Compression Porometry of Battery Separators, *Journal of Power Sources*, Vol. 80, 1999, p.46.
2. A.W. Adamson, *Physical Chemistry of Surfaces*, Interscience, 1967.
3. Vibhor Gupta and A.K. Jena, Substitution of Alcohol in Porometers for Bubble Point Determination, *Advances in Filtration and Separation Technology*, American Filtration and Separation Society, Vol.13b, 1999, p. 833.
4. A.E. Scheidegger, *The Physics of Flow through Porous Media*, Macmillan, 1957.
5. Gerard Kraus, J.W. Ross and L.A. Girifalco, Surface Area Analysis by Means of Gas Flow Methods. I. Steady State Flow in Porous Media, *Phys. Chem.*, Vol. 57, 1953, p. 330.
6. Vibhor Gupta and A.K. Jena, Effects of Compression on Porosity of Filter Materials, *Advances in Filtration and Separation Technology*, American Filtration and Separation Society, Vol. 13a, 1999, p.10.
7. Akshaya Jena and Krishna Gupta, 'Evaluation of Permeability of Strong Chemicals at Elevated Temperatures and High Pressures', *The 2002 17th Annual Battery Conference on Applications and Advances*, California State University, Long Beach, California, Proceedings, December 2001, IEEE Catalog Number 02TH8576..
8. V. Perna and A. K. Jena., In-plane and through-plane porosities in Nonwovens, *Proceedings of 1999 TAPPI Nonwovens Conference*, 1999, p. 177.
9. A. Jena and K. Gupta, Analyse der Porendurchmesser von Mehrschichtfiltermitteln, *F&S Filtrieren und Separieren*, Jahrgang 16, Nr. 1, 2002, p. 13.
10. Nalini Gupta and Akshaya Jena, Determining the Pore Structure of Individual Layers of Multi-layered Ceramic Composites, *Ceramic Industry*, Vol. 151, Issue 2, February 2001, p. 24.
11. Akshaya Jena and Krishna Gupta, Measurement of Pore Volume and Flow through Porous Materials, *Materials Testing MP Materialprüfung*, Jahrgang 44, Juni, 2002, p.243.

12. Akshaya Jena and Krishna Gupta, 'Materials Pore-sight - Testing pore volume and flow through porous materials', Materials World, The Journal of the Institute of Materials, Vol. 10, Number 2, February, 2002, p.20.
13. Akshaya Jena and Krishna Gupta, A Novel Mercury Free Technique for Determination of Pore Volume, Pore Size and Liquid Permeability', PM Science & Technology Briefs, Vol. 4, No. 1, 2002, p. 5.
14. S. Lowell and E. Shields, Powder Surface Area and Porosity, Chapman Hall Publication, 1984.
15. Akshaya Jena, Howard Sanders, Jamie Miller and Rick Wimberly, Comparison of Mercury Porosimetry and Flow Porometry for the Testing of Battery Separator Materials, IEEE 01TH8533, p. 71.
16. Akshaya Jena and Krishna Gupta, Use of Multiple Test Techniques for Evaluation of Complex Pore Structures, Proceedings of the 15th Annual Technical Conference, April 9-12, 2002, Galveston. Texas, American Filtration & Separation Society, 2002. p. 05.
17. Akshaya Jena and Krishna Gupta, Homogeneity of Pore Structure of Filtration Media, Proceedings of the 15th Annual Technical Conference, April 9-12, 2002, Galveston. Texas, American Filtration & Separation Society, 2002. p. 02.
18. Akshaya Jena and Krishna Gupta, Design of Composite Filtration Media Using Flow Porometry, Book of Papers, INTC 2000, INDA, Cary, North Carolina, USA, 2000, p. 10.0.